PAPER

Optimization of the catalytic production of methyl stearate by applying response surface Box–Behnken design: an intensified green option for high-cetane biofuel manufacture†

Federico Manuel Reyes-Cruz, [ID] [a] Juana Deisy Santamaría-Juárez,[a] Manuel Sánchez-Cantú [ID] *[a] and Roberto Quintana-Solórzano [ID] *[b]

To enhance the efficiency of processes by decreasing the reaction severity and energy consumption, and reducing the equipment size, facilities' space and operation cost, process intensification is an increasingly used option in the chemical industry. Within this framework and in agreement with some of the green chemistry principles (design for energy efficiency and use of renewable feedstocks), this work deals with the implementation of high-shear mixing (HSM) to intensify the homogeneous esterification of stearic acid (SA) with methanol to methyl stearate, a high-cetane number alkyl ester suitable to be added into biofuel streams. The response surface Box–Behnken design (BBD) is applied to quantify the main effects and two-way interactions of four key input reaction factors: methanol : SA ratio (7–16 mol mol^{-1}), catalyst mass (0.25–4.0 wt%), temperature (40–60 °C), time (1–12 min), and to approximate the optimal conditions on the intensified SA esterification. The statistical BBD results indicates that the four linear effects, two of the four possible quadratic effects (catalyst mass and temperature) and only one (catalyst mass–time) of the six existing two-way interactions are statistically relevant at the 95% confidence level. Catalyst mass is the most influencing factor in the reaction, followed by methanol : SA ratio, temperature, and time. The proposed second-order regression model predicts that the intensified esterification requires only 12 min to practically convert all SA (99% ± 6.8%) running the reaction at 12.4 methanol : SA ratio, 4 wt% catalyst mass, 60 °C and 500 rpm, a value experimentally validated (93.2% ± 0.7%). Under these conditions and with the assistance of HSM, the typical reaction length of conventional heterogeneous and homogeneous-phase esterification processes decreases from 5 to 117 and 35 to 90 times, respectively.

Introduction

Energy consumption worldwide is growing year by year to satisfy the increasing needs of humankind. Although the use of diverse alternative energy forms such as solar, wind, and geothermic are gradually increasing, fossil fuels will still have a relevant role in industrial development worldwide. The key sectors of demand for fossil fuels are well identified and specifically pertain to land, air and maritime transportation as well as to the production of petrochemical compounds, which are gaining importance.[1–3] In the context of fuels used for land transportation, particular attention has been paid towards diesel

engine motors as they are highly reliable for moving oversized loads in places like cities, country roads and marine regions. Notwithstanding, during diesel combustion in diesel-powered engines, several toxic emissions such as CO_x, SO_x, NO_x, particulate matter and unburned hydrocarbons are generated in relatively large amounts.[4] From the beginning, biofuels and bioadditives have been decidedly considered alternatives to gradually mitigate the environmental impact caused by the combustion of petroleum-based fuels. Among them, much attention has been centred on biodiesel (BD) due to its similarities to diesel. BD consists of a mixture of alkyl esters that are produced by the transesterification of vegetable oils or animal greases or by the catalytic esterification of fatty acids with a short chain alcohol (generally methanol).[5]

The physicochemical properties of BD are closely related to their quality and, therefore, they can be conveniently adjusted by modifying its native chemical composition. In this respect, the cetane number (CN) of BD, which is a key property for determining diesel's quality, is notably influenced by the nature

[a]*Facultad de Ingeniería Química, Benemérita Universidad Autónoma de Puebla, Avenida San Claudio y 18 Sur, C.P. 72570 Puebla, Puebla, Mexico. E-mail: manuel. sanchez@correo.buap.mx*

[b]*Instituto Mexicano del Petróleo, Eje Central Lázaro Cárdenas Norte 152, Ciudad de México, 07730, Mexico. E-mail: rquintana@imp.mx*

† Electronic supplementary information (ESI) available. See DOI: https://doi.org/10.1039/d4ra02750g

of the constituent triglyceride or free fatty acids. Giakoumis,[6] who reported values of CN for distinct triglyceride sources such as soybean, palm, coconut oil, beef tallow and chicken fat, commented on the effect of the triglyceride profile on the CN values. Yanowitz et al.,[7] in turn, published a compilation of 299 CN values for pure chemical compounds. Interestingly, it has been reported that alkyl esters prepared from stearic, palmitic, myristic or lauric acid display the highest CN values. Among them, methyl stearate (MST) exhibited the highest CN ranging from 75.6 to 95.6; therefore, MST production is identified as a reasonable alternative for extensively using this compound as a high CN biofuel or even as a CN bioadditive for low CN fuels.

Concerning MST production, it is well known that this alkyl ester can be synthesized *via* the esterification of stearic acid (SA) with methanol following homogeneous, heterogeneous, or enzymatic routes; however, the number of reports dealing with the synthesis of MST is scarce contrasting to what is found for other alkyl esters. Regarding the heterogeneous route for MST production, some catalysts including montmorillonite-based clays,[8–11] Amberlyst-15,[12] Nb_2O_5,[13] tin zirconium oxide,[14] amidoximated polyacrylonitrile ion exchange fibres,[15] carbon-based catalyst[16] and sulfated ZrO_2–SiO_2 (ref. 17) have been tested. Although the heterogeneous route seems to be the most attractive, it has set disadvantages that are basically ascribed to the required reaction severity, *i.e.*, the relatively high temperature (60–160 °C) and large reaction time (−23 h), the large excess of alcohol related to the fatty acid amount (1–150), the catalyst amount (0.07–30%) and the pretreatment with acids for activation prior to the reaction; all this certainly complicates the route to scale-up. Regarding the enzymatic route, the use of alcohols such as ethanol[18,19] and *n*-butanol[19] have been reported in the esterification of SA. Concerning the homogeneous synthesis of MST, two reports were identified in the literature: one using $AlCl_3$ as a catalyst that converted 98% of SA conversion running at 18 h of reaction time, 24 : 1 molar ratio, 5% catalyst and 110 °C,[20] and a second one using sulfuric acid as the catalyst in which SA conversion amounted to 97% at 60 °C after 7 h of reaction time, adding 6% catalyst and 60 : 3 mol ratio of alcohol : fatty acid.[17] In homogenous esterification, advantageously, SA conversion was almost complete; nonetheless, a very large reaction time is usually required.

An attractive alternative to overcome the above-mentioned drawbacks regarding the large reaction time of conventional processes pertains to the incorporation of intensification options.[21] Recently, the application of the high-shear mixing (HSM) technology displayed promising results for intensifying the transesterification of triglycerides,[22,23] esterification of fatty acids,[24] production of azidoesteroids[25] and anionic clays,[26] respectively. Being little mass transfer restricted and requiring lower reaction severity (temperature, residence time, *etc.*) to run compared to non-assisted counterparts,[27] processes assisted by HSM are expected to be more efficient and require simplified facilities. Thus, it is necessary to perform a quantitative and systematic assessment of the reactor operating variables in the route to scale up and optimize intensified processes. To this end, the application of formal design of experiments (DoE) is a suitable, effective, cheap, and fast option as it provides

valuable information through a reasonable number of well-selected set of experimental runs.

Among several studies on MST production are available in the scientific literature, a very small number of publications deal with the application of DoE are found: two report relatively simple 2^k factorial designs[9,28] and only one applies a Box–Behnken design for a heterogeneous reaction yet is limited to two factors.[10] The so-called response surface designs such Central Composite (CCD) and Box–Behnken (BBD) are suitable for investigating processes dealing with more than three factors require a reasonable number of experiments and can be used for optimization.[29] BBD includes experimental points positioned in the middle of the edges, thus providing a better description of non-linear effects compared to CCD.[29–32] In this context, our publication aims to rigorously quantify, by applying response surface BBD, the concomitant effect of four principal reaction variables (methanol to SA molar ratio, catalyst mass, temperature and time) on the HSM-assisted liquid phase acid-catalysed esterification of SA with methanol to MST.

Material and methods

Chemicals

SA was acquired from Fermont Lab (94.2%), whilst methyl alcohol (95%), isopropyl alcohol (95%), phenolphthalein solution (1%) and sulfuric acid (95%) were purchased from Meyer. Potassium hydroxide in the form of pellets (85%) was procured from Golden Bell and the deuterated chloroform used in the ${}^1H$ NMR analyses (99.8 atom %D) was acquired from Sigma-Aldrich. All reactants were used without further purification. Deionized water (25 MΩ cm) was supplied by a water deionizing plant installed at the facilities of the BUAP University.

Materials characterization

The acid value measurement (AV) was carried out by the titration method reported by Zhang et al.,[33] using eqn (1).

$$AV = \frac{(P_s - P_b) \times -P_m \times -P_w}{W} mg \ KOH \ g^{-1} \qquad (1)$$

where P_s and P_b are the millilitres of potassium hydroxide solution required in the titration and blank, respectively, P_m is the molarity of the potassium hydroxide solution, P_w denotes the molecular mass of potassium hydroxide, and W corresponds to the aliquot mass taken for titration.

To verify the formation of MST upon the reaction, the product of the esterification of SA with methanol from an experiment carried out at methanol : SA ratio = 11.5, catalyst mass = 2.98 g, temperature = 60 °C and time = 12 min, under stirring at 500 rpm was analysed by proton nuclear magnetic resonance (${}^1H$ NMR); SA was also characterized by this analytical technique. The reaction products were dissolved in deuterated chloroform and then analysed in a Bruker Avance III 500 MHz NMR spectrometer. The chemical shifts (δ) were expressed in ppm (parts per million).

Esterification reaction of SA

The experimental synthesis of MST was conducted in the batch mode based on the procedure reported previously.[24]

(i) SA was heated at 40 °C, methanol was added, and, afterwards, the resulting mixture was heated to the required reaction temperature.

(ii) Next, sulfuric acid was added to the SA and methanol mixture in the required quantity to catalyse the rection, and.

(iii) The resulting admixture was subsequently dispersed for the defined reaction time at 500 rpm in a ROSS HSM-100 LCI high shear mixer equipped with a slotted stator head dispersion attachment *vide* Section S1 in the ESI.† The mixing rate was defined through preliminary experiments, which are displayed in detail in the ESI.† Upon the reaction, the unreacted methanol was removed in a rotavapor at reduced pressure. The methanol-free sample was then washed with hot water to eliminate the remaining catalyst (see Section S1 in the ESI†). The aqueous fraction was subsequently removed using a separation funnel, producing a sample consisting of unconverted SA and MST, which was then titrated to determine the AV value.[33] Finally, the percentage of SA converted during the esterification reaction was determined according with eqn (2), which is related to the AV, where AV_{Sai} is the AV before the reaction) and AV_{Saf} is the AV after the reaction.[34]

$$X_{SA}\% = \frac{AV_{Sai} - AV_{Saf}}{AV_{Sai}} \times 100 \qquad (2)$$

Box–Behnken design

The factors and corresponding operation intervals of the BBD applied to investigate the HSM-assisted liquid phase acid-catalysed esterification of SA with methanol to MST were as follows: methanol : SA ratio (7–16 mol mol^{-1}), catalyst mass (0.25–4.0 g), temperature (40–60 °C), and time (1–12 min). In a similar homogeneous reaction system,[24] the incorporation of HSM led to a low stirring speed-sensitive process. Preliminary SA esterification to MST experiments confirmed this behaviour (see Fig. S1 in the ESI†); therefore, the stirring speed was set to 500 rpm and removed from the design experiments, thus leading to a more manageable BBD. The four remaining factors are independent variables influencing the catalyst performance, kinetics and reactor operation, with the respective intervals being defined by combining the state-of-art information,

experimental set-up limitations, preliminary experimental results (*vide* Fig. S2 in ESI†) and chemical equilibrium data.

Table 1 includes a summary of the four factors of the BBD, the corresponding full and short names for the purposes of this work, and the respective levels in accordance with typical DoE codification wherein the low, central or middle and high levels are denoted by "−1", "0", and "+1", respectively. Notice that three levels per factor are needed. The explicit BBD experimental matrix containing the specific reaction conditions per experiment is displayed in Table S2 in the ESI.† The total number of experimental points (N) is given by $2k (k − 1) + n_c$, where $k = 4$ represents the number of factors and $n_c = 3$ denotes the replicates at the middle point. Thus, N amounted to 27, corresponding to the summation of 24 base runs resulting from the combination of the midpoints of edges of the process region and at the centre point, plus 3 replicated runs at the centre point;[29–32] which are used to compute the so-called pure error.[35,36] Likewise, aimed at finding the set of reaction conditions that maximize SA conversion, response surface methodology was applied fitting the raw experimental data to a full second-order regression model.

Results and discussion

Proton nuclear magnetic resonance (^{1}H NMR) characterization

^{1}H NMR analysis was used to verify the formation of MTS in the esterification reaction between SA and methanol catalyzed by sulfuric acid. To this end, two samples were analysed, where was SA used as the starting material and the product recovered upon reaction under the following conditions: methanol : SA ratio = 11.5, catalyst mass = 2.98 g, temperature = 60 °C, time = 12 min, and stirring speed = 500 rpm. The corresponding ^{1}H-NMR spectra are shown in Fig. 1. Indicated with number in the SA ^{1}H NMR spectrum in Fig. 1a, the set of observed characteristic chemical shifts, δ (ppm) correspond to 2.37–2.32 (t, 2H, –CH$_2$–) −1, 1.66–1.60 (m, 2H, –CH$_2$–) −2, 1.32–1.25 (m, 28H, –CH$_2$–) −3, 0.89–0.87 (t, 3H, –CH$_3$) −4. The difference between

Table 1 Box–Behnken design experimental limits and coding factors in the SA esterification with methanol to MST

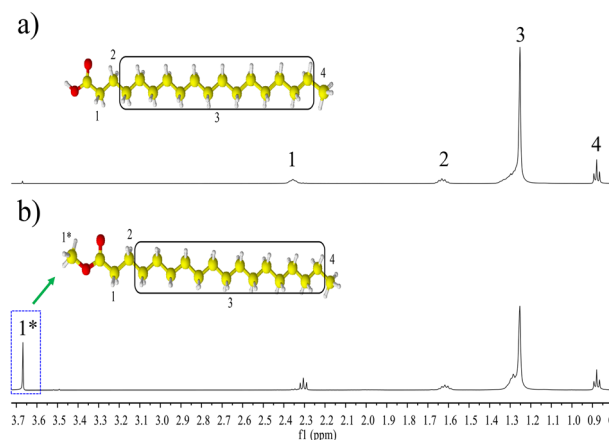| BBD factors coding		BBD factors level		
		Low	Middle	High
Full name	Short name	−1	0	+1
Methanol : SA ratio, mol mol^{-1}	MeOH : SA	7.0	11.5	16.0
Catalyst mass, wt%	Cat	0.25	2.125	4.0
Temperature, °C	Temp	40	50	60
Time, min	Time	1.0	6.5	12.0

Fig. 1 ^{1}H NMR spectra: (a) stearic acid (SA) used as a reagent in the esterification reaction, and (b) methyl stearate (MST) produced in the reaction of SA with methanol.

the ^{1}H NMR spectrum of SA and that of MST (see Fig. 1b) is clearly noticed by the signal appearing at 3.67 ppm, which is ascribed to the protons of the methoxy group (s, 3H –OCH$_3$)–1*, thereby evidencing the presence of a methyl ester.[15,20]

Graphical assessment of the main effects and interactions

A qualitative valuation of the main effects of the individual DoE factors and the possible two-way interactions was done by the visual inspection of the so-called main effect and interaction graphs. Built using the available raw experimental results, these graphs provide valuable information to have an initial view of the relative magnitude and nature of the various treatments in the BBD.[37,38] In the case of main effects, they show how the average response value varies as the level of the factor in the BBD gradually increases from level "−1" to "0" and then from level "0" to "+1". For a multi-factor DoE, the existence of interaction between the pair of factors is common;[38] in this sense, the corresponding graphs are useful to visualize whether or not the effect of the first factor is influenced by the level of the second factor.

Fig. 2 displays the main effect graphs for the four factors in the BBD. They contain three points comprising the average value of SA conversion of experiments operated at the levels "−1", "0" and "+1" of a given factor, independent of the level of the other three factors in the DoE.[33,34] The shape of the line (straight or curve) joining the three points in the graphs indicates the nature (linear or non-linear) of the main effect, while the slope of the line (positive, neutral, or negative) denotes the direction and intensity of the main effect on the response. From Fig. 2a, it is noted that the main effect of MeOH : SA ratio on the response is almost linear and positive and has a moderate intensity. Fig. 2b suggests that the main effect of catalyst mass on SA conversion is positive and non-linear, showing a concave down increasing trend as the response value is more notably affected when augmenting the factor level from "−1" to "0". Fig. 2c and d are very similar, indicating that both temperature and time have a weak average positive and non-linear effect, displaying a concave up increasing trend.

Based on a comparison of the four main effect graphs in Fig. 2, qualitatively, the catalyst mass appears as the most influencing factor in the process, followed by the MeOH : SA ratio, temperature and time. Moreover, as most of the points in the graphs in Fig. 2 do not align to a straight line, quadratic effects (or curvature) are expected to be important in the process with a magnitude that must be quantified through a rigorous formal statistical analysis, as will be presented in further sections.

Regarding binary interactions, Fig. 3 depicts the six possible two-way interaction graphs of the BBD. These graphs contain three series of average response values of experiments run at the
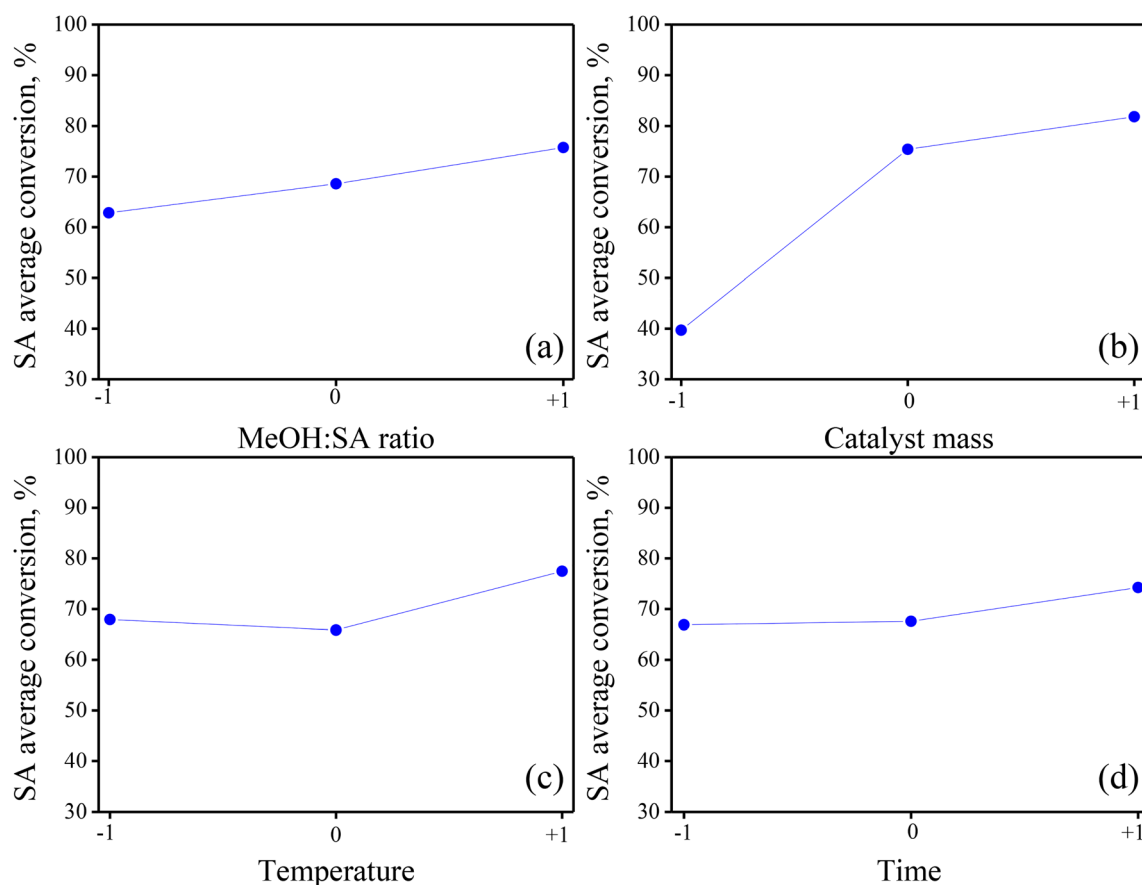

Fig. 2 Main effects graphs for the four factors accounted for in the BBD: (a) methanol : SA ratio, (b) catalyst mass, (c) temperature and (d) time.
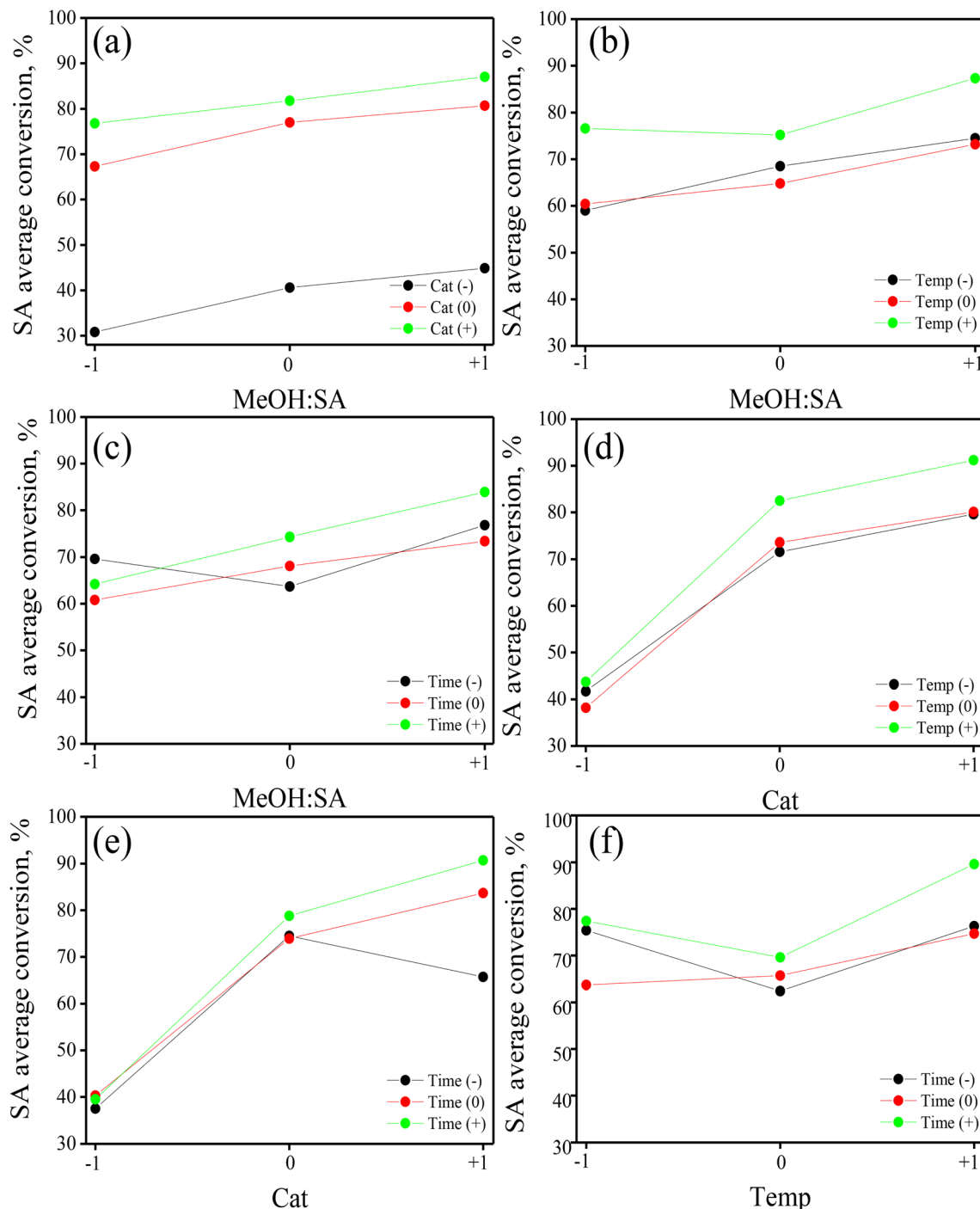
Fig. 3 Interaction graphs of the four factors BBD applied to the acid-catalyzed esterification of SA with methanol: (a) methanol : SA ratio–catalyst mass, (b) methanol : SA ratio–temperature, (c) methanol : SA ratio–time, (d) catalyst mass–temperature, (e) catalyst mass–time, and (f) temperature–time.

levels "−1", "0" and "+1" of one of the factors while gradually varying the level of a second factor, irrespective of the level of the two remaining factors.[37,38] There is evidence of a binary interaction when the slope of three trendlines changes; in fact, the more different the slopes, the stronger the interaction between the factors. In this sense, the three trendlines in Fig. 3a and d are practically parallel, suggesting that the binary

interactions methanol : SA ratio–temperature and catalyst mass – time would not be relevant in the reaction. Conversely, the binary interactions methanol : SA ratio–temperature (Fig. 3b), methanol : SA ratio–time (Fig. 3c), catalyst mass–time (Fig. 3e), and temperature–time (Fig. 3f) are expected to be relevant as the slope of the three trendlines in the corresponding graphs and even the intercept are different, as occurs in the case of Fig. 3f.

The application of formal statistical tools will generate appropriate information to quantify these interactions and determine their statistical significance at a given probability level, *vide infra*.

Fitting the BBD results with the full regression model

When applying response surface design of experiments such as CCD or BBD, a mathematical equation is used to predict the experimental response values as a function of the factors of the DoE.[38] As the visual inspection of the main effects and binary interaction graphs (see Fig. 2 and 3) suggests that curvature may be important for some of the BBD factors, a second-order polynomial was incorporated. Notice that this mathematical expression, which is generally represented by eqn (3), explicitly includes linear and quadratic effects and two-way interactions. In eqn (3), $\hat{Y}$ represents the value response, x_i and x_j are the factors or independent variables with i (or j) = 1, 2,…, k.[37,38] The parameter β_o is defined as the intercept with the ordinate axis, and the parameters β_i, β_{ii} and β_{ij} symbolize, accordingly, the regression parameters ascribed to linear, quadratic and two-way interaction effects.

$$\hat{Y} = \beta_o + \sum_{i=1}^{k} \beta_i x_i + \sum_{i=1}^{k} \beta_{ii} x_i^2 + \sum_{i=1}^{k} \sum_{j=1;\ i \neq j}^{k} \beta_{ij} x_i x_j \quad (3)$$

The BBD used in this work contains four factors (*i.e.*, $k = 4$) and, therefore, the explicit form of the full second-order polynomial model of eqn (3) contains 15 adjustable parameters (β_0, β_1,…, β_4, β_{11},…, β_{44}, β_{12},…, β_{34}), whilst the independent variables in eqn (3) correspond to x_1, x_2, x_3 and x_4 and denote the factors methanol : SA ratio, catalyst mass, temperature, and time, respectively. The model parameters were numerically estimated *via* regression with the software Data Fit 7.1 using the 27 experimental SA conversion values as input (see ESI Table S1†). The main values of the parameters in the full regression model are displayed in Table 2, which also includes, as a footnote, the relevant statistical information to assess the quality of the numerical fitting and model adequacy. Notice that the

multiple determination coefficient (R^2) was as high as 0.9768, indicating that 98% of the data variability is explained by the model, while for the *F*-test: $F_{0,\text{reg}}$ (=36.21) > $F_{\text{crit,reg}}$ (=2.5342) and the *p*-test: *p* value for lack of fit (=0.000) < 0.05; that said, there is evidence that the full regression model exhibits no lack of fit.[39]

To verify graphically the adequacy of the full regression model to simulate the experimental results for SA conversion, the so-called parity and residuals plots were built (see Fig. 4). The parity plot in Fig. 4a shows that the predicted response values matched well with the experimental counterparts as the corresponding points are close and align well to the 45° reference line in the graph. Likewise, the plot in Fig. 4b indicates that the residual values distribution (model-predicted SA conversion minus experimental SA conversion) is random with respect to the model-predicted SA conversion values.

Variance analysis (ANOVA) and individual confidence limits

The application of graphical tools only provided a preliminary understanding of the main effect and interaction of the factors accounted in the BBD; therefore, the implementation of formal statistical tools is required to determine their magnitude and significance at a defined probability level. The ANOVA, which is based on the values of sum of squares (SS) and mean squares (MS) for the different treatments (*i.e.*, main/quadratic effects and interactions),[37–39] offers valuable information on their relative magnitude and statistical significance. Notwithstanding, as ANOVA does not offer information about the absolute magnitude and direction of various treatments, it must be complemented with the calculation of the individual confidence limits (ICL), which comprises the estimate of the treatment and its margin of error at the same probability level used in ANOVA.

In Table 3, the ANOVA results of the BBD are summarized for the linear and quadratic effects as well as the two-way interactions. To determine the statistical significance of the treatments, the *F*-test was applied, and the *p*-values were computed. The *F*-test incorporates the *F* value (F_0), which is obtained by dividing the MS of the treatment by the MS of the total error. For any treatment and the total error, the MS values are computed by dividing the SS by the degrees of freedom. F_0 is next contrasted with the tabulated *F*-value or *F* critical (F_{crit}), which is obtained at a given probability level (usually 95% or 0.95, or a significance level of 5% or 0.05) and the degrees of freedom of the treatment (v_1) and the total error (v_2). The *p*-value, in turn, was obtained from F_0 and the degrees of freedom v_1 and v_2. The treatment is statistically significant when $F_0 > F_{\text{crit}}$ or *p*-value < 0.05.

From what is said above, the information in Table 3 indicates that in the four linear effects (catalyst mass, methanol : SA ratio, temperature and time), two of the four quadratic effects (catalyst mass and temperature) and only one of the six binary interactions (catalyst mass–time) are statistically significant at the 95% probability as their corresponding F_0 is greater than the F_{crit} counterpart, and the *p*-values are larger than 0.05. Considering that the magnitude of F_0 depends on the impact of

Table 2 Main parameters estimated numerically for the full second-order regression model used to predict the values of SA conversion during its esterification with methanol to MST[a]

Model parameter	Main value	Model parameter	Main value
β_0	110.364×10^0	—	—
β_1	3.437×10^0	β_{44}	2.684×10^{-2}
β_2	19.295×10^0	β_{12}	-1.146×10^{-1}
β_3	-3.823×10^0	β_{13}	-2.684×10^{-2}
β_4	-4.898×10^0	β_{14}	1.258×10^{-1}
β_{11}	-5.403×10^{-2}	β_{23}	1.284×10^{-1}
β_{22}	-3.948×10^0	β_{24}	5.569×10^{-1}
β_{33}	3.997×10^{-2}	β_{34}	5.174×10^{-2}

[a] Regression sum of squares (SS_{Reg}) = 8046.28; lack-of-fit (LoF) sum of squares (SS_{LoF}) = 189.35; error sum of squares (SS_{Error}) = 190.43; multiple determination coefficient (R^2) = 0.9768; $F_{0,\text{reg}}$ = 36.21 with $F_{\text{crit,reg}}$ (0.05,14,12) = 2.5342, $F_{0,\text{reg}} > F_{\text{crit,reg}}$.; *p* value for LoF = 0.000 (<0.05).
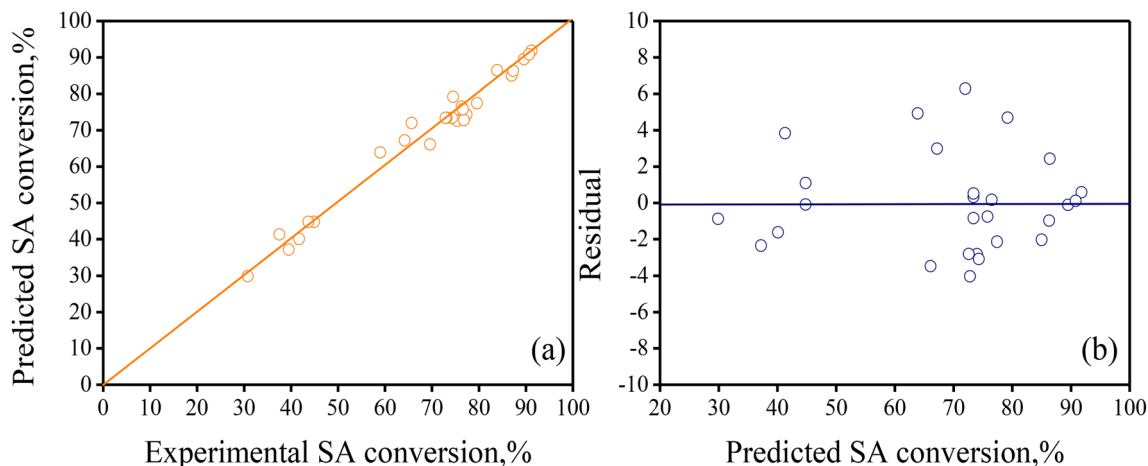
Fig. 4 (a) Parity plot contrasting computed SA conversion *vs.* experimental SA conversion, and (b) residuals as a function of the predicted SA conversion values. The full regression model in eqn (4) with the parameters in Table 2 was used to calculate the response values.

Table 3 Summary of the ANOVA results for the four factors accounted for the BBD applied to the HSM-assisted acid esterification of SA with methanol to MST

Treatment	DF	SS	MS	F_0	F_{crit} at 95% prob.	*p*-value	$F_0 > F_{crit}$ or *p*-value < 0.05
Full model	14	8046.29	574.73	36.22	2.64	0.000	Sign.
MeOH : SA	1	500.28	500.28	31.52	4.75	0.000	Sign.
Cat	1	5328.98	5328.98	335.79	4.75	0.000	Sign.
Temp	1	272.85	272.85	17.19	4.75	0.001	Sign.
Time	1	162.07	162.07	10.21	4.75	0.008	Sign.
$(MeOH : SA)^2$	1	6.39	6.39	0.4	4.75	0.538	No sign.
$(Cat)^2$	1	1027.59	1027.59	64.75	4.75	0.000	Sign.
$(Temp)^2$	1	85.23	85.23	5.37	4.75	0.039	Sign.
$(Time)^2$	1	3.52	3.52	0.22	4.75	0.646	No sign.
MeOH : SA–cat	1	3.74	3.74	0.24	4.75	0.636	No sign.
MeOH : SA–temp	1	5.77	5.77	0.36	4.75	0.558	No sign.
MeOH : SA–time	1	38.79	38.79	2.44	4.75	0.144	No sign.
Cat–temp	1	23.2	23.2	1.46	4.75	0.250	No sign.
Cat–time	1	131.93	131.93	8.31	4.75	0.014	Sign.
Temp–time	1	32.39	32.39	2.04	4.75	0.179	No sign.
Total error	12	190.44	15.87				
Lack-of-fit	10	189.36	18.94	35.27	4.1028	0.028	
Pure error	2	1.07	0.54				
Total	26	8236.73					

the treatment on the response, it is noted that the linear effect of the catalyst mass is, by far, the most influencing variable (F_0 = 335.79 *vs.* F_{crit} = 4.75) in the SA esterification reaction. With respect to the two quadratic effects that were statistically significant, the one of the catalyst mass is notably larger (F_0 = 64.7 *vs.* F_{crit} = 4.75) than that of temperature (F_0 = 5.37 *vs.* F_{crit} = 4.75).

To determine the absolute magnitude and direction of the treatments in the BBD, the main value of linear effects and quadratic effects as well as two-way interactions with the corresponding t-based ICL at the 95% of probability were computed and are summarized in Table 4. Notice that the ICL involves the *t*-distribution (or *t*-student) value and the standard error (SE), the latter computed from the MS of the total error

and the sample size. When there is a zero in the ICL of a treatment, one can conclude that it is not statistically significant at the selected probability level.[38,40,41] Table 4 also contains the so-called standardized effect designated *T*-value, which is equal to the main value of the treatment divided by the SE, which provides complementary information to identify if a treatment is statistically significant or not. The *T*-value was used to obtain the *p*-values at the probability level indicated before, giving statistical results that are fully consistent to that displayed in Table 3.

Notice that the ICL of the four linear effects do not contain any zero and their *p*-values that are lower than 0.05, which indicate that they are statistically significant. Likewise, these effects are positive, showing that by increasing the level of the

Table 4 Main value of linear and quadratic effects as well as binary interactions with confidence limits at the 95% probability level for the four factors BBD model applied to the HSM-assisted acid esterification of SA with methanol to MST

Treatment	ICL (main value $\pm$ 2.179 SE)^a	T-value	p-value
MeOH : SA	12.92 ± 5.01	5.61	0.000
Cat	42.14 ± 5.01	18.32	0.000
Temp	9.54 ± 5.01	4.15	0.001
Time	7.34 ± 5.01	3.20	0.008
$(\text{MeOH : SA})^2$	-2.18 ± 7.50	-0.63	0.538
$(\text{Cat})^2$	-27.76 ± 7.50	-8.05	0.000
$(\text{Temp})^2$	8.00 ± 7.50	2.32	0.039
$(\text{Time})^2$	1.62 ± 7.50	0.47	0.646
MeOH : SA–cat	-1.94 ± 8.67	-0.49	0.636
MeOH : SA–temp	-2.40 ± 8.67	-0.60	0.558
MeOH : SA–time	6.22 ± 8.67	1.56	0.144
Cat–temp	4.82 ± 8.67	1.21	0.250
Cat–time	11.48 ± 8.67	2.88	0.014
Temp–time	5.70 ± 8.67	1.43	0.179

^{a} The number 2.179 was taken from the t-student distribution at the 95% probability and the degrees of freedom of the total error (=12) in Table 3.

Table 5 Main parameters and confidence intervals at the 95% probability level for the reduced second-order regression model used to predict the values of SA conversion during its esterification with methanol to MST^a

Parameter	Main value
β_0	96.318×10^0
β_1	1.4348×10^0
β_2	24.313×10^0
β_3	-3.591×10^0
β_4	-5.152×10^{-1}
β_{22}	-3.928×10^0
β_{33}	4.068×10^{-2}
β_{24}	5.569×10^{-1}

^{a} $SS_{\text{Reg}} = 7927.7$, $SS_{\text{LoF}} = 190.60$; $SS_{\text{Error}} = 309.0$; $F_{0,\text{reg}} = 69.65$ with $F_{\text{crit,reg (0.05,19,7)}} = 3.45$, $F_{0 \text{ reg}} > F_{\text{crit,reg}}$ (R^2) = 0.9624, p-value for LoF = 0.000 (<0.05).

factor, the value of the response increases with the catalyst mass being the factor with the most intense linear effect on the response and time corresponding to the factor with the least important impact on the response values. Regarding the quadratic effects, the ones associated with catalyst mass and temperature are statistically significant (no zero in the ICL), in agreement with what was found in the ANOVA, with the former being negative and the latter being positive in accordance with the concavity of the trendline in Fig. 2b and c. Moreover, only the interaction catalyst mass–time is statistically significant and positive, which indicates that the positive effect of catalyst mass on the response is more pronounced as time increases.

Fitting the BBD results with the reduced regression model

From the detailed revision of the ANOVA results in Table 3, combined with the assessment of the ICL values in Table 4, it was found that the quadratic effect of the methanol : SA ratio and time and the binary interactions methanol : SA ratio–catalyst mass, methanol : SA ratio–temperature, methanol : SA ratio–time, catalyst mass–temperature, and temperature–time were not statistically significant at 95% of probability. Thus, they can be removed out from the full regression model to give a simplified expression, denoted as the reduced regression model.[42] In the case of our BBD, this reduced model is represented by eqn (4), which only contains 8 adjustable parameters that were estimated again *via* regression using the 47 available experimental BBD runs, as was done formerly for the full regression model.

$$\hat{Y} = \beta_o + \beta_{1\times1} + \beta_{2\times2} + \beta_{3\times3} + \beta_{4\times4} + \beta_{22\times22} + \beta_{33\times32} + \beta_{24\times2\times4} \quad (4)$$

Table 5 presents the main value of the 8 parameters of eqn (4) and includes relevant statistical information as a footnote. Based on this statistical information, $R^2 = 0.9624$, $F_{\text{c reg}}$ (=69.65)

$> F_{\text{crit}}$ (=3.45) and the p-value for LoF = 0.000 (<0.05), along with the parity and residual plots depicted in Fig. 5, it is concluded that the reduced regression model adequately predicts the experimental BBD data and is suitable for updating the ANOVA and ICL values of the statistically significant treatments.

Table 6 summarizes the ANOVA results, which were obtained by applying the reduced regression model to adjust the BBD data. As expected, all the treatments, *i.e.*, linear and quadratic effects, as well as binary interactions incorporated to the reduced regression model are statistically significant at the 95% probability level upon fulfilling that $F_0 > F_{\text{crit.}}$ and p-value > 0.05 correspondingly. Table 7, in turn, presents the ICL at the 95% of probability of the treatments retained in the reduced regression model; none of the ICL are zero, indicating that all the treatments are statistically significant, which is consistent with the ANOVA results displayed in Table 6. Summarizing: (i) the four linear effects are positive and that associated with the mass of catalyst is the most influencing on SA conversion, (ii) the quadratic effect of catalyst mass is negative and that of temperature is positive, producing an opposite concavity in the corresponding response surface plots (*vide* the response surface graphs in the coming section), and (iii) only one interaction (catalyst mass–time) is significant, albeit with a relatively low magnitude based on the narrowness of the ICL.

Response surface graphs

The response surface graphs (RSG), which are tridimensional graphs constructed with the corresponding regression models, represent a useful tool to visualize the evolution of the response value in terms of the simultaneous changes in the two factors at a time. The RSG also contain bidimensional contour plots that include lines connecting the points of iso-response values, from which the intensity of the binary interactions can be confirmed.[43,44] For a DoE with more than two factors, the factors that are not displayed in the graph are set to a fixed value conventionally to the middle point "0" of the factor interval.[39,40] Constructed using the second order reduced regression model (see eqn (4) and Table 5), Fig. 6 shows the complete set of RSG of the BBD, which were graphed using the software Origin 9.0. For
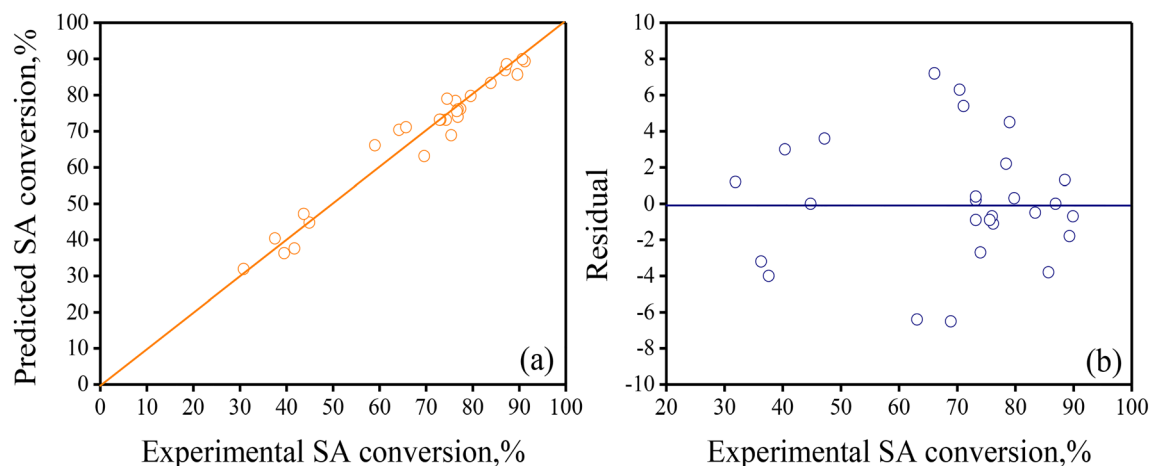
Fig. 5 (a) Parity plot contrasting computed SA conversion *vs.* experimental SA conversion, and (b) residuals as a function of the predicted SA conversion values. The reduced regression model in eqn (5) with the parameters in Table 5 was used to calculate the response values.

Table 6 Summary of the ANOVA results for the four factors accounted for the BBD represented by the reduced regression model applied in the HSM-assisted acid esterification of SA with methanol to MST

Treatment	DF	SS	MS	F_0	F_{crit} at 95% prob.	p-value	$F_0 > F_{crit}$ or p-value < 0.05
Full model	7	7927.72	1132.53	69.64	2.54	0.000	Sign.
MeOH : SA	1	500.28	500.28	30.76	4.38	0.000	Sign.
Cat	1	5328.98	5328.98	327.66	4.38	0.000	Sign.
Temp	1	272.85	272.85	16.78	4.38	0.001	Sign.
Time	1	162.07	162.07	9.96	4.38	0.005	Sign.
$(Cat)^2$	1	1220.6	1220.6	75.05	4.38	0.000	Sign.
$(Temp)^2$	1	105.92	105.92	6.51	4.38	0.019	Sign.
Cat–time	1	131.93	131.93	8.11	4.38	0.010	Sign.
Total error	19	309.01	16.26				
Lack-of-fit	17	307.93	18.11	33.74	19.4	0.029	
Pure error	2	1.07	0.54				
Total	26	8236.73					

Table 7 Magnitude of linear and quadratic effects as well as binary interactions with confidence limits at the 95% probability level for the four factors BBD represented by the reduced regression model applied to the HSM-assisted acid esterification of SA with methanol to MST

Treatment	ICL (main value ± 2.093 SE)[a]	T-value	p-value
MeOH : SA	12.92 ± 4.86	5.55	0.000
Cat	42.14 ± 4.86	18.10	0.000
Temp	9.54 ± 4.86	4.1	0.001
Time	7.34 ± 4.86	3.16	0.005
$(Cat)^2$	−27.62 ± 6.66	−8.66	0.000
$(Temp)^2$	8.14 ± 6.66	2.55	0.019
Cat–time	11.48 ± 8.46	2.85	0.010

[a] The number 2.093 was taken from the *t*-test tables at the 95% probability ($\alpha = 0.05$) and the degrees of freedom of the total error (=19) from Table 6.

the factors not displayed in the RSG, their value was set to at 11.5 mol mol^{-1}, 2.125 wt%, 50 °C, and 6.5 min for methanol : SA ratio, catalyst mass, temperature, and time, respectively, the factors' middle point in the BBD (see Table 1).

As the regression model in eqn (4) contains linear and two quadratic terms, the shape of the SRP can be pure planar (*e.g.*, Fig. 6c, which includes methanol:SA and time as independent variables) and curve (*e.g.*, Fig. 6a, b and f, which accounts for catalyst mass or temperature and methanol : SA or time as independent variables). Regarding their topology,[45] the observed RSG are rising ridge (Fig. 6a and e), planar (Fig. 6c), saddle (Fig. 6d) and falling ridge-like (Fig. 6b and f). It is also noted that the RSG, including catalyst mass and the BBD factor that exhibited a negative quadratic effect, are concave downward (Fig. 6a and e), whereas for those incorporating the temperature, the BBD factor that displayed a positive quadratic effect, are concave upward (Fig. 6b and f). The non-linear effect of the catalyst mass and/or temperature on the response is confirmed by the shape of the contour plots in Fig. 6a, b, d, e and f as their corresponding contour lines are curved. Conversely, the contour lines in the contour plots in Fig. 6c are straight, confirming the linear effect of methanol : SA and time on the response. An inspection of the iso-response contour lines allows the relative influence of the various factors in the response to be quickly
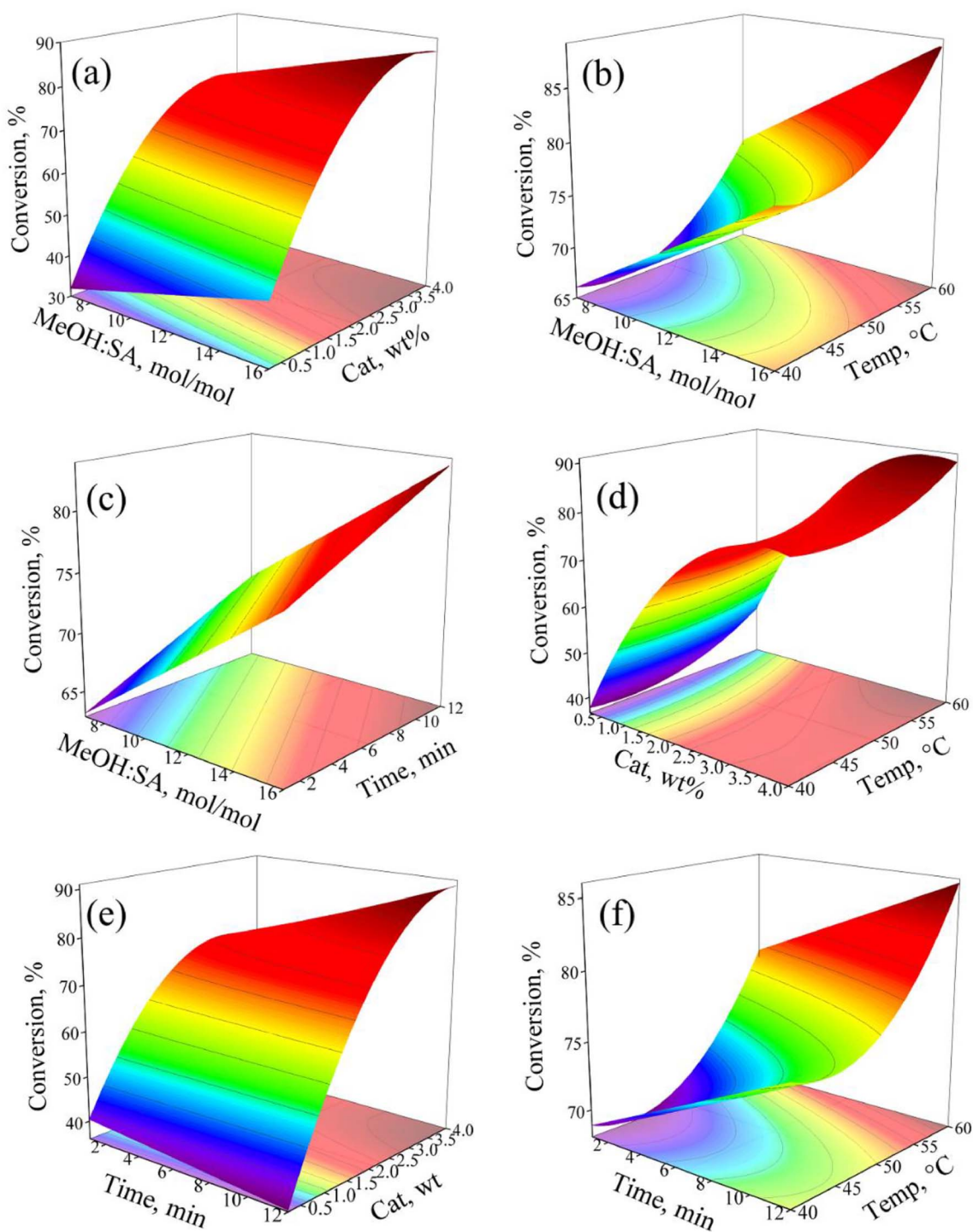
Fig. 6 Response surface graphs with contour plots constructed from the reduced regression model (see eqn (5)) that includes the parameters in Table 5. Two factors are included in the graph, and the value of the other two factors was set at the center point "0" in the BBD.

visualized. Thus, in Fig. 6a, d and e, small changes in the catalyst mass make the contour lines move to regions of large response values. Though the response value also increases with augmenting methanol : SA, temperature and time and the iso-response contour lines displace to higher values, and the positive effect of these three factors is notably lower than the one displayed by the catalyst mass.

In the SRP in Fig. 6, it is also noticed that the operation at the upper limit of the two factors in the plots leads to the largest SA conversion, a behaviour that can be explained in terms of the main effects assessment outlined in the previous sections. For instance, it is observed in Fig. 6a that SA conversion was as high as 87% when running the reaction at 4 wt% of catalyst mass and 16 mol mol^{-1} of methanol : SA ratio (recall that temperature and

Table 8 Comparative reaction condition reported in the state-of-the-art for the esterification of SA with methanol to MST

Type of reaction	Catalyst	Reaction conditions					Times of reaction severity reduction using the HSM intensified esterification reported in this work		
		Temperature, °C	Time, h	Catalyst mass, wt%	Alcohol : fatty acid, mol : mol	SA conversion, %	Temperature	Time	Catalyst mass
Heterogeneous	MMT KSF/0 (ref. 8)	150	4	10	2.06 : 1	96	2.5	20	2.5
	MMT-PO$_4$ (ref. 9)	160	2	12	12 : 1	96.6	2.7	10	3.0
	MMT K10 (ref. 9)	160	2	12	12 : 1	94.1	2.7	10	3.0
	Cu^{2+}–MMT K10 (ref. 10)	80	1.03	30	8 : 1	87.05	1.3	5.15	7.5
	Fe-MMT K10 (ref. 11)	80	3	30	1.06 : 1	75	1.3	15	7.5
	Amberlyst-15 (ref. 12)	110	5	7	1 : 1	Above 50	1.8	25	1.8
	Niobium-oxide[12]	110	10	7	1 : 1	50	1.8	50	1.8
	Nb$_2$O$_5$ (ref. 13)	110	23.3	5	1 : 1	40	1.8	116.5	1.3
	Tin zirconium oxide[14]	120	1	0.07	150 : 1	74	2.0	5	0.02
	Amidoximated polyacrylonitrile ion exchange fibres[15]	90	3	1.5	35.5 : 1	95.35	1.5	15	0.4
Homogeneous	ZrO$_2$–SiO$_2$ (ref. 17)	60	7	6	60 : 3	91	Same	35	1.5
	AlCl$_3$ (ref. 20)	110	18	5	24 : 1	98	1.8	90	1.3
	Sulfuric acid[17]	60	7	6	60 : 3	97	Same	35	1.5

time were set to the middle level "0" in the BBD: 50 °C and 6.5 min, *vide* Table 2). Interestingly, the reaction time required in the HSM-intensified SA esterification with methanol was considerably smaller than the typical reaction time values reported in the literature either for heterogeneous[8,13,14,17] or homogeneous[17,20] non-intensified processes, as can be verified from the information displayed in Table 8. In fact, the ANOVA (Tables 3 and 6) and the ICL results (see Tables 4 and 7) indicate that time is, among the four factors accounted for in the BBD, the least influencing independent variable in the SA conversion, an issue that appears to be related to the incorporation of HSM into the esterification process. Clearly, by assisting the liquid phase esterification reaction with high shear rotor stator mixer, the reaction less mass-transfer limited the contact between reactants and catalyst is more intimate, and the liquid droplets are smaller and better dispersed, thus ultimately leading to a more efficient process.[22–24,46] These results are of great relevance as energy saving can be envisaged by reducing the reaction severity in time (as well as temperature and catalyst amount), which may ultimately positively impact the process economy.

For multifactorial response surface DoE, identifying the values of the factors that maximizes the response within the corresponding experiment region is not trivial and requires a numerical approximation. From a ridge max analysis using the reduced regression model as the input, the maximum SA conversion amounted to 99 ± 6.8%, running at 12.4 mol mol^{-1} methanol : SA ratio, 4 g catalyst mass, 60 °C temperature and 12 min time upon stirring at 500 rpm. With the aim to validate this result, three replicated experiments at these reaction conditions were conducted giving, as an average, an SA conversion value of 93.2 ± 0.7%.

Conclusions

The response surface methodology was successfully applied to experimentally/numerically determine the set of conditions that favours the MST production *via* the liquid phase acid-catalysed esterification of SA acid with methanol. Interestingly, the said homogeneous esterification was intensified by assisting it with high shear mixing (HSM). The use of a four-factor (catalyst mass, methanol : SA ratio, temperature, and time) response surface Box–Behnken design (BBD) allowed us their main effect (linear and quadratic) and two-way interactions on SA conversion to be measured and statistically assessed. In the first stage, the inspection of the constructed main effects and interaction plots was useful for a preliminary view of the relative importance of BBD factors and their nature. By combining numerical and statistical tools (ANOVA and individual confidence limits), the statistically relevant treatments in the BBD (linear and quadratic effect as well as binary interactions) at the 95% probability were identified. The treatments evolved as follows: (i) the four linear effects were positive, (ii) the interaction catalyst mass–time was positive, and (iii) the quadratic effect of catalyst mass and temperature were negative and positive, respectively. The catalyst mass was the most influencing reaction variable, then methanol : SA ratio, temperature, and time.

The projection of the fitted reduced regression model indicates the intensified process requires only 12 min to almost fully convert SA ($99 \pm 6.8\%$ conversion) when operating at 12.4 methanol : SA ratio, 4 wt% catalyst mass, 60 °C and 500 rpm, a value that was experimentally validated ($93.2 \pm 0.7\%$). In comparison with the available state-of-the-art reports, the reaction severity (time in particular) drastically reduced, giving evidence that HSM is a promising option for intensifying green chemistry reactions, visualising noticeable technical, economic, and environmental benefits. As immediate future actions to increase the maturity level of this technology, increasing the scale of the reaction set-up and implementing experiments under more realistic conditions that implies the use of commercial reagents would be two of the key steps.

Abbreviations

-1	Factor's low level in the BBD
$+1$	Factor's high level in the BBD
0	Factor's central or middle point in the CCD
^{1}H NMR	Proton nuclear magnetic resonance
ANOVA	Analysis of variance
AV	Acid value, (mg KOH) g^{-1}
AV_{SAf}	Acid value after reaction, (mg KOH) g^{-1}
AV_{SAi}	Acid value before reaction, (mg KOH) g^{-1}
BD	Biodiesel
BBD	Box–Behnken design
Cat	Catalyst mass, wt%
CI	Confidence interval
CN	Cetane number
cp	Total number of replicates at the central point
DF	Degrees of freedom
DoE	Design of experiments
Fc	Computed F value in the Fisher's statistical test
$F_{c\ reg}$	F value for the regression in the Fisher's statistical test
F_{crit}	Critical F value in the Fisher's test
F-test	Fisher's statistical test
F value	Value generated from Fisher's statistical test
HSM	High-shear mixing
k	Number of factors or independent variables in the DoE
LoF	Lack-of-fit
MeOH : SA	Methanol : stearic acid molar ratio, mol mol^{-1}
MS	Mean squares
MS_{Error}	Total error of mean sum of squares
MS_{reg}	Mean sum of squares of the regression
MST	Methyl stearate
N	Total number of experiments in the BBD
P_b	Solution required for blank solvent titration, ml
P_m	Molarity of the potassium hydroxide solution, mol l^{-1}
P_s	Potassium hydroxide solution, ml
P_w	Molecular mass of potassium hydroxide
p-value	Probability value used to apply the statistical test
R^2	Multiple correlation coefficient in the regression analysis
Reg	Regression
RSG	Response surface graphs
SA	Stearic acid
SE	Standard error
SS	Sum of squares
SS_{Error}	Error sum of squares
SS_{LoF}	Lack-of-fit sum of squares
SS_{Reg}	Regression sum of squares
Temp	Temperature, °C
Time	Time, min
W	Mass of titration, g
x_i, x_j	Factor (independent variable) coding in regression model
X_{SA}	SA converted during the esterification reaction,%
$\hat{Y}$	Predicted response value by the regression model

Greek letters

α	Significance or probability level used for the F-test and p-value
β_0	Intercept parameter in the regression model
β_i	Parameters related to linear effects in the regression model
β_{ii}	Parameters related to quadratic effects in the regression model
β_{ij}	Parameters related to the two-way interactions in the regression model

Author contributions

Conceptualization: R. Q. S. and M. S. C.; methodology: R. Q. S., M. S. C. and F. M. R. C.; formal analysis: R. Q. S., M. S. C. and F. M. R. C.; investigation: R. Q. S., M. S. C. and F. M. R. C.; data curation: R. Q. S., M. S. C. and F. M. R. C.; ^{1}H NMR analysis: J. D. S. J.; writing—original draft preparation, F. M. R. C., R. Q. S. and M. S. C.; writing—review and editing, F. M. R. C., R. Q. S. and M. S. C.; visualization: R. Q. S. and F. M. R. C.; supervision: R. Q. S. and M. S. C.; project administration: R. Q. S. and M. S. C.; funding acquisition: M. S. C.

Conflicts of interest

There are no conflicts to declare.

Acknowledgements

References

1 P. G. Levi and J. M. Cullen, *Environ. Sci. Technol.*, 2018, **52**, 1725–1734.
2 E. Işıklı, N. Aydın, L. Bilgili and A. Toprak, *J. Cleaner Prod.*, 2020, **275**, 124142.
3 E. Khalife, M. Tabatabaei, A. Demirbas and M. Aghbashlo, *Prog. Energy Combust. Sci.*, 2017, **59**, 32–78.

4 T. Kegl, A. Kovač Kralj, B. Kegl and M. Kegl, *Prog. Energy Combust. Sci.*, 2021, **83**, 100897.

5 Z. Khan, F. Javed, Z. Shamair, A. Hafeez, T. Fazal, A. Aslam, W. B. Zimmerman and F. Rehman, *J. Ind. Eng. Chem.*, 2021, **103**, 80–101.

6 E. G. Giakoumis, *Renewable energy*, 2013, **50**, 858–878.

7 J. Yanowitz, E. M. A. Ratcliff, R. L. Mccormick, J. D. Taylor and M. J. Murphy Battelle, *Compendium of Experimental Cetane Numbers*, 2014.

8 S. Bouguerra Neji, M. Trabelsi and M. H. Frikha, *Energies*, 2009, **2**, 1107–1117.

9 L. Zatta, E. J. M. Paiva, M. L. Corazza, F. Wypych and L. P. Ramos, *Energy Fuels*, 2014, **28**, 5834–5840.

10 E. A. Almadani, F. W. Harun, S. M. Radzi and S. K. Muhamad, *Bull. Chem. React. Eng. Catal.*, 2018, **13**, 187–195.

11 O. Al, F. W. Harun, E. A. Almadani, S. M. Radzi and F. W. Harun, *Int. J. Agric. Crop Sci.*, 2016, **12**, 62–67.

12 M. Banchero and G. Gozzelino, *Energies*, 2018, **11**, 1843.

13 M. Banchero and G. Gozzelino, *Chem. Eng. Res. Des.*, 2015, **100**, 292–301.

14 S. M. Ibrahim, *Renewable Energy*, 2021, **173**, 151–163.

15 R. A. Ahmed, S. Rashid and K. Huddersman, *J. Ind. Eng. Chem.*, 2023, **119**, 550–573.

16 P. Sangsiri, N. Laosiripojana, W. Laosiripojana and P. Daorattanachai, *ACS Omega*, 2022, **7**, 40025–40033.

17 K. Saravanan, B. Tyagi and H. C. Bajaj, *J. Porous Mater.*, 2016, **23**, 937–946.

18 H. Nakaya, K. Nakamura and O. Miyawaki, *J. Am. Oil Chem. Soc.*, 2002, **79**, 23–27.

19 G. N. Pereira, J. P. Holz, P. P. Giovannini, J. V. Oliveira, D. de Oliveira and L. A. Lerin, *Biocatal. Agric. Biotechnol.*, 2018, **16**, 373–377.

20 N. U. Soriano, R. Venditti and D. S. Argyropoulos, *Fuel*, 2009, **88**, 560–565.

21 Z. Qian, Q. Chen and I. E. Grossmann, *Comput.-Aided Chem. Eng.*, 2018, **44**, 2377–2382.

22 M. Sánchez-Cantú, L. M. Pérez-Díaz, M. Morales-Téllez, I. Martínez-Santamaría, J. C. Hilario-Martínez and J. Sandoval-Ramírez, *Fuel*, 2017, **189**, 436–439.

23 M. Sánchez-Cantú, M. Morales Téllez, L. M. Pérez-Díaz, R. Zeferino-Díaz, J. C. Hilario-Martínez and J. Sandoval-Ramírez, *Renewable Energy*, 2019, **130**, 174–181.

24 F. M. Reyes-Cruz, R. Quintana-Solórzano and M. Sánchez-Cantú, *Int. J. Energy Res.*, 2022, **46**, 19548–19565.

25 R. Zeferino-Díaz, J. C. Hilario-Martínez, M. Sánchez-Cantú, M. A. Fernández-Herrera and J. Sandoval-Ramirez, *Green Chem.*, 2019, **21**, 1417–1420.

26 J. S. Valente, M. S. Cantu and F. Figueras, *Chem. Mater.*, 2008, **20**, 1230–1232.

27 B. Ai, J. Guo, S. Zhao, W. Li, M. Zhou and J. Zhang, *Ind. Eng. Chem. Res.*, 2021, **60**, 4498–4509.

28 J. De Araújo Gonaçalves, A. L. D. Ramos, L. L. L. Rocha, A. K. Domingos, R. S. Monteiro, J. S. Peres, N. C. Furtado, C. A. Taft and D. A. G. Aranda, *J. Phys. Org. Chem.*, 2011, **24**, 54–64.

29 X. Shen, G. Zhang and B. Bjerg, *Energy Build.*, 2013, **62**, 570–580.

30 B. Ait-Amir, P. Pougnet and A. El Hami, *Embedded Mechatronic Systems*, 2015, **2**, 151–179.

31 A. Jankovic, G. Chaudhary and F. Goia, *Energy Build.*, 2021, **250**, 111298.

32 S. L. C. Ferreira, R. E. Bruns, H. S. Ferreira, G. D. Matos, J. M. David, G. C. Brandão, E. G. P. da Silva, L. A. Portugal, P. S. dos Reis, A. S. Souza and W. N. L. dos Santos, *Anal. Chim. Acta*, 2007, **597**, 179–186.

33 J. Zhang, M. Lu, F. Ren, G. Knothe and Q. Tu, *J. Am. Oil Chem. Soc.*, 2019, **96**, 1083–1091.

34 R. Chakraborty and E. Mandal, *J. Taiwan Inst. Chem. Eng.*, 2015, **50**, 93–99.

35 I. Miličević, N. Štirmer and D. Bjegović, *Optimizing the Concrete Mixture Made with Recycled Aggregate Using Experiment Design*, 2011.

36 N. Aslan and Y. Cebeci, *Fuel*, 2007, **86**, 90–97.

37 G. E. P. Box and K. B. Wilson, *J. R. Stat. Soc. Series B.*, 1591, **13**, 1–45.

38 D. C. Montgomery, *Design and analysis of experiments*, 2012.

39 P. Qiu, M. Cui, K. Kang, B. Park, Y. Son, E. Khim, M. Jang and J. Khim, *Cent. Eur. J. Chem.*, 2014, **12**, 164–172.

40 J. S. Valente, R. Quintana-Solórzano, H. Armendáriz-Herrera, G. Barragán-Rodríguez and J. M. López-Nieto, *Ind. Eng. Chem. Res.*, 2014, **53**, 1775–1786.

41 G. E. P. Box, J. S. Hunter and W. G. Hunter, *Statistics for Experimenters: An Introduction to Design, Data Analysis and Model Building*, 1978.

42 E. E. Feistauer, J. F. Dos Santos and S. T. Amancio-Filho, *Weld. World.*, 2020, **64**, 1481–1495.

43 S. A. Younis, A. Abd-Elaziz and A. I. Hashem, *RSC Adv.*, 2016, **6**, 89367–89379.

44 W. Chen, P. Yin, H. Chen and Z. Wang, *Ind. Eng. Chem. Res.*, 2012, **51**, 5402–5407.

45 R. H. Myers, D. C. Montgomery and C. M. Anderson-Cook, *Response Surface Methodology. Process and Product Optimization Using Designed Experiments*, 2016.

46 J. Zhang, S. Xu and W. Li, *Chem. Eng. Process.*, 2012, **57–58**, 25–41.